Received: 12 June 2020 | Revised: 17 November 2020 | Accepted: 30 November 2020

DOI: 10.1002/kin.21464

INTERNATIONAL JOURNAL OF CHEMICAL KINETICS WILEY

ARTICLE

Mechanistic scrutiny of the oxidations of thiol-containing drugs cysteamine and D-penicillamine by *cis*-diamminetetrachloroplatinum(IV)

Li Zhou[1] | **Tiejian Li**[2,3] | **Ying Sun**[2] | **Hongwu Tian**[3] | **Cunxiu Gao**[2] | **Chunli Liu**[1] | **Lingli Kong**[1] | **Guimin Zhang**[2,3] | **Tiesheng Shi**[1]

[1] College of Chemistry, Chemical Engineering and Materials Science, Zaozhuang University, Zaozhuang, Shandong Province 277160, China

[2] National Engineering Technology Center of Chirality Pharmaceuticals, Lunan Pharmaceutical Group Co., Ltd., Linyi, Shandong Province 276006, China

[3] Shandong New Time Pharmaceutical Co., Ltd., Feixian, Shandong Province 273400, China

Correspondence
Guimin Zhang, National Engineering Technology Center of Chirality Pharmaceuticals, Lunan Pharmaceutical Group Co., Ltd., Linyi 276006, Shandong Province, China.
Email: lnzhangguimin@lunan.cn
Tiesheng Shi, College of Chemistry, Chemical Engineering and Materials Science, Zaozhuang University, Zaozhuang 277160, Shandong Province, China.
Email: rock@uzz.edu.cn

Li Zhou and Tiejian Li contributed equally to this work.

Funding information
Critical R&D Plans of Shandong Province (Major Scientific Innovation Projects), Grant/Award Number: 2019JZZY010516; Natural Science Foundation of Shandong Province, Grant/Award Number: ZR2019MB015

Abstract

Cysteamine (CA) and D-penicillamine (Pen) are the thiol-containing drugs and good antioxidants. Their reactions with a cisplatin Pt(IV) prodrug *cis*-diamminetetrachloroplatinum(IV) (*cis*-$[Pt(NH_3)_2Cl_4]$) were investigated by use of rapid scan, stopped-flow, and mass spectral techniques. The kinetic traces are biphasic in nature, encompassing a faster reduction of *cis*-$[Pt(NH_3)_2Cl_4]$ to cisplatin followed by slow substitutions on cisplatin. The reduction reactions were demonstrated to follow overall second-order kinetics over a wide pH range. The observed second-order rate constants versus pH profiles were established at 25.0°C and 1.0 M ionic strength, indicating a huge increase of reaction rate with the increase of pH. However, the oxidations of CA and Pen by *cis*-$[Pt(NH_3)_2Cl_4]$ displayed different reaction stoichiometric ratios as revealed by the spectrophotometric titration experiments. Accordingly, CA was oxidized to CA-disulfide while Pen-sulfinic acid and Pen-disulfide were identified as the major products in the case of Pen via mass spectral analysis. The above similarities and differences are rationalized in terms of the proposed reaction mechanisms, which encompass similar rate-determining reactions for both CA and Pen, but involve disparate and faster followed-up reactions. Rate constants of the rate determining were derived at 25.0°C and 1.0 M ionic strength. A consequent species reactivity analysis revealed that the species $-SCH_2CH_2NH_3^+$ of CA and the species $^+H_3NCH(COO^-)CMe_2S^-$ of Pen played a predominant role toward the reduction of *cis*-$[Pt(NH_3)_2Cl_4]$ from pH 5 to 8, which also is a critical pH region for most of drugs.

KEYWORDS
cis-$[Pt(NH_3)_2Cl_4]$, cysteamine, D-penicillamine, kinetics, mechanism, reduction

1 | INTRODUCTION

Among the thiol-containing drugs, cysteamine (CA) bearing the simplest structure was approved for the treatment of cystinosis; it removes cystine that builds up in cells of people with the disease.[1–3] In addition, it has been in clinical trials for Parkinson's disease, malaria, radiation sickness, neurodegenerative disorders, neuropsychiatric

disorders, and cancer treatment.[3] Biologically, it has a function of promoting the transport of L-cysteine into cells that can be further used to synthesize glutathione, which is one of the most potent intracellular antioxidants.[3] D-Penicillamine (Pen) is also a thiol-containing drug, but its thiol group is structurally hindered by the two adjacent methyl groups. Pen is a medication used primarily for the treatment of Wilson's disease;[4,5] it is also used for people with kidney stones, rheumatoid, and various heavy metal poisonings.[4,5] The anticancer effect of Pen has also been exploited.[6] Moreover, the antioxidative properties of CA and Pen related to some pharmacological processes have been pursued as exemplified by the research works in references[7–9]; this is not hard to understand since both CA and Pen are good antioxidants due to the thiol group in the drugs.

Not surprisingly, a number of kinetic and mechanistic investigations on the oxidations of CA and Pen by various types of oxidants have been performed in order to have a better understanding of their antioxidative properties.[10–15] These investigations have clearly unraveled that the kinetic rate laws and the derived reaction mechanisms are totally diversified, depending largely upon the nature of the oxidants[10–15]; and based on the investigations, it is almost impossible to predict an oxidation mechanism when a new oxidant is considered. In the last few years, we have been focusing on the mechanistic elucidations for some redox reactions concerning a few important drugs.[16–20] We thus performed a detailed kinetic analysis of oxidation reactions of CA and Pen by *cis*-diamminetetrachloroplatinum(IV) (*cis*-$[Pt(NH_3)_2Cl_4]$) and divulge the results in the present work. *cis*-$[Pt(NH_3)_2Cl_4]$ is an anticancer active Pt(IV) compound and is in fact a cisplatin prodrug since it can be easily reduced to cisplatin (*cis*-$[Pt(NH_3)_2Cl_2]$)[21–23]; its reductive activation processes by some biologically important molecules and by an electrochemical approach have been studied.[17,19,23–25] On the other hand, it was reported that mechanistically, a combination of Pen and platinum anticancer drugs synergistically inhibited tumor growth.[26] The above-mentioned impetuses promoted us to undertake the present study, enabling us to have a mechanistic scrutiny on the oxidation reactions and to unravel the mechanistic similarities and differences. The structures of *cis*-$[Pt(NH_3)_2Cl_4]$, *cis*-$[Pt(NH_3)_2Cl_2]$, CA and Pen are shown in Figure 1.

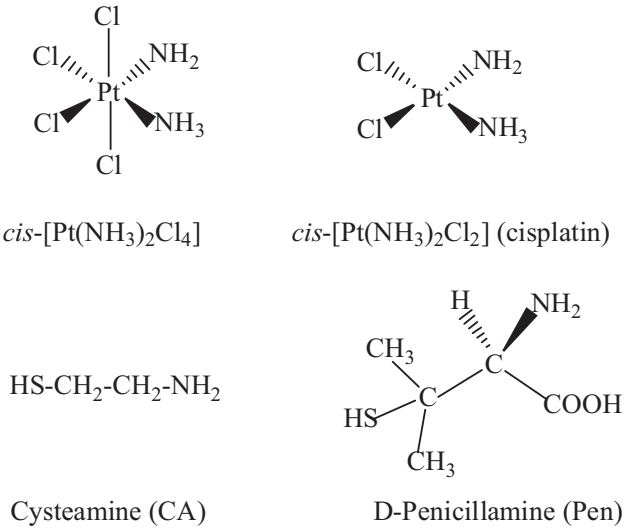

cis-$[Pt(NH_3)_2Cl_4]$ *cis*-$[Pt(NH_3)_2Cl_2]$ (cisplatin)

Cysteamine (CA) D-Penicillamine (Pen)

FIGURE 1 Structures of *cis*-$[Pt(NH_3)_2Cl_4]$ and *cis*-$[Pt(NH_3)_2Cl_2]$ and of thiol-containing drugs cysteamine and D-penicillamine

2 | EXPERIMENTAL

2.1 | Materials

Cysteamine hydrochloride (CA), Pen, *cis*-$[Pt(NH_3)_2Cl_4]$), and *cis*-$[Pt(NH_3)_2Cl_2]$ in their purest forms were obtained from Sigma–Aldrich (St. Louis, MO, USA). Acetic acid, sodium acetate, sodium chloride, hydrochloric acid, concentrated *o*-phosphoric acid (ca 85% solution), sodium dihydrogen-phosphate, disodium hydrogen phosphate, trisodium phosphate dodecahydrate, sodium bicarbonate, sodium carbonate, sodium perchlorate, and 0.100 M NaOH standard solution were purchased as the purest forms available either from Fisher Scientific (Fisher Branch in Shanghai, China) or from Alfa Aesar (Alfa Aesar Branch in Shanghai, China). These chemicals were used directly without further purification. For pH meter calibrations, standard buffers of pH 4.00, 7.00, and 10.00 were purchased from Fisher Scientific. Doubly distilled water was employed for preparations of all the solutions used in this work.

2.2 | Buffer solutions

Buffering pairs of H_3PO_4/NaH_2PO_4, HAc/NaHc, NaH_2PO_4/Na_2HPO_4, $NaHCO_3/Na_2CO_3$, and Na_2HPO_4/Na_3PO_4 (0.15-0.2 M) were prepared to cover a pH range of $2.47 \leq pH \leq 11.81$. All the buffer solutions contained 0.10 M of NaCl and 2.0 mM of EDTA; sodium perchlorate was used to adjust the ion strength (μ) of buffers to 1.0 M. The addition of NaCl was to suppress the hydrolysis of the Pt(IV) complex. The role of EDTA in the buffers was to complex trace amounts of metal ions such as Cu(II) and Fe(III), eliminating or minimizing the catalytic effects of the metal ions in the thiol oxidation processes.[13,27–29] An Accumet Basic AB150 Plus pH meter equipped with an Accumet combination pH electrode (Fisher Scientific,

Pittsburgh, PA, USA) was utilized to measure the pH of buffer solutions; the electrode was calibrated just before the measurements by use of the standard buffers of pH 4.00, 7.00 and 10.00.

2.3 | Rapid scan spectra and kinetic data collection

An Applied Photophysics SX-20 stopped-flow spectrometer (Applied Photophysics Ltd., Leatherhead, UK) was employed for kinetic measurements and for recording the rapid scan spectra. The stopped-flow spectrometer was connected to a water bath circulation from a thermostat (Lauda Alpha RA8; Delran, NJ, USA); temperature could be controlled to ±0.1°C. A stock solution of 1.0 mM *cis*-$[Pt(NH_3)_2Cl_4]$ was prepared daily by dissolving the desired amount of the Pt(IV) complex in a solution containing 0.90 M $NaClO_4$, 0.09 M NaCl, and 0.01 M HCl; these solutions were only used for a few hours. A stock solution of CA/Pen (20-30 mM) was prepared just before the kinetic measurements by dissolving a certain amount of CA/Pen in a specific buffer; the stock solution was bubbled with nitrogen for 10 min and was only used for a couple of hours. Solutions of CA/Pen and of the Pt(IV) complex for kinetic measurements were prepared, respectively, by adding an appropriate amount of the Pt(IV) stock solution and of CA/Pen stock solution to the buffer of the same pH. Those solutions were bubbled for 5 min with nitrogen before loading onto the stopped-flow machine. Reactions were started by mixing equal volumes of CA/Pen and Pt(IV) solutions directly in the stopped-flow machine; pseudo first-order conditions were fulfilled by utilizing CA/Pen being at least 10-fold excess. The software provided by the Applied Photophysics in the control system was employed to simulate the kinetic traces.

2.4 | Electronic spectra and absorption measurements

Electronic spectra and absorption measurements at room temperature were performed on a TU-1900 spectrophotometer and 1.00 cm quartz cells were used (all from Beijing Persee, Inc., Beijing, China).

2.5 | Mass spectral measurements

A reaction mixture of 1.0 mM *cis*-$[Pt(NH_3)_2Cl_4]$ with 10 mM CA in 10 mM acetic acid after a reaction time of about 0.5 h was run on a high resolution mass spectrometer (Apex Ultra 7.0T FT-ICR; Bruker Daltonik, Bremen, Germany) with an ESI of positive ionization mode. On the other hand, an Agilent 1200/6310 ion trap mass spectrometer with an ESI was employed for recording the mass spectra for a reaction mixture of 1.0 mM *cis*-$[Pt(NH_3)_2Cl_4]$ with 8 mM Pen in 10 mM acetic acid after a reaction time of about 0.5; both positive and negative modes of ionization were run.

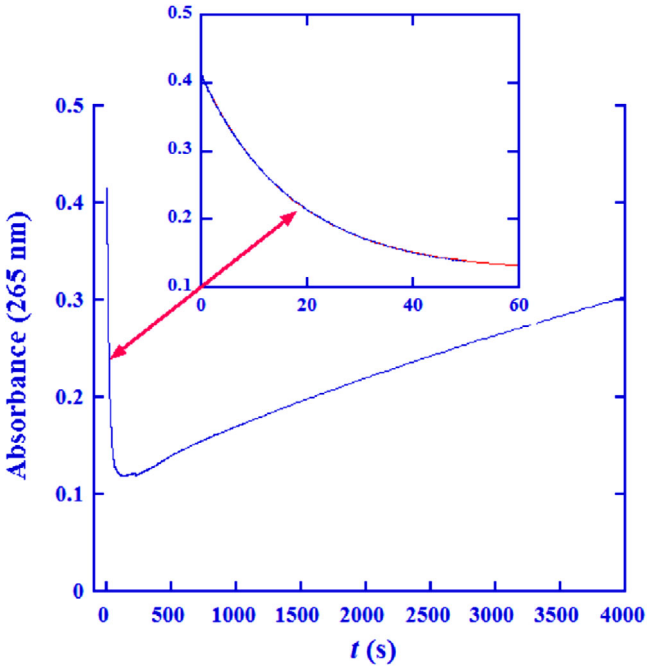

FIGURE 2 A kinetic trace acquired at 265 nm for the reaction between *cis*-$[Pt(NH_3)_2Cl_4]$ and CA by the stopped-flow spectrometer under the reaction conditions: [Pt(IV)] = 0.20 mM, $[CA]_{tot}$ = 2.00 mM, pH 4.52 buffer, 25.0°C, and 1.0 M ionic strength. Insert: The kinetic trace is enlarged to show the initial phase between 0 to 50 s; the red curve was resulted from a theoretical simulation of the experimental data by Equation (1) [Color figure can be viewed at wileyonlinelibrary.com]

3 | RESULTS AND DISCUSSION

3.1 | Kinetic traces

As a control, the electronic spectra of 0.10 mM *cis*-$[Pt(NH_3)_2Cl_4]$, 0.10 mM *cis*-$[Pt(NH_3)_2Cl_2]$, 1.0 mM CA, and 1.0 mM Pen recorded in an HAc/NaAc buffer of pH 4.42 are given in Figure S1 in Supplementary Materials (SM). The general kinetic traces under pseudo first-order reaction conditions, that is, the thiol drug total concentrations $[thiol]_{tot}$ being ≥ 10•[Pt(IV)], were investigated. A kinetic trace for the oxidation of CA by *cis*-$[Pt(NH_3)_2Cl_4]$ under a set of reaction conditions is shown in Figure 2 displaying a biphasic nature. The initial absorption decline of the kinetic trace, being enlarged and shown in the insert of Figure 2, is designated to the reduction of *cis*-$[Pt(NH_3)_2Cl_4]$

to cisplatin; while the second phase, that is, the subsequent absorption increase, is much slower, which can be assigned to the substitution of the coordination chloride(s) in cisplatin by the excess CA in the reaction mixture.[19] In the oxidation of Pen by the Pt(IV) compound, similar biphasic kinetic traces were also observed, cf Figures S2 and S3 in the SM. Since the kinetic trace is basically separable on the time scale, the initial kinetic phase was well-simulated by a single exponential equation (cf Equation 1), where A_t, A_0, and A_∞ pertain to the

$$A_t = (A_0 - A_\infty)\exp(-k_{obsd}t) + A_\infty \quad (1)$$

absorbances at time t, zero and infinity, respectively.[30] In the equation, k_{obsd} stands for the pseudo first-order rate constant, and the value A_∞ can hardly be acquired directly from the kinetic trace due to the subsequent reaction, but is obtainable through the simulation. The simulated result is also shown in the insert of Figure 2, indicating that the reduction phase is indeed first-order in [Pt(IV)]. Since the substitution reactions on cisplatin proceed slowly,[31] and are not directly related to the antioxidative properties of the drugs, our attention in this work is paid to the redox processes.

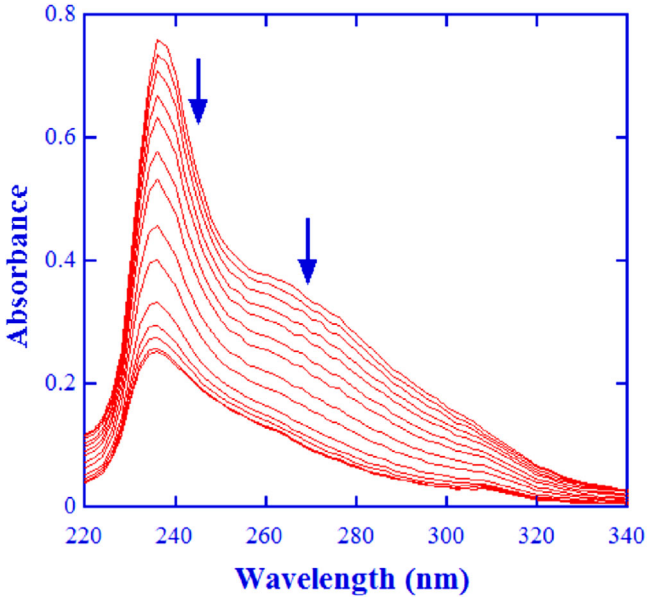

FIGURE 3 Time-resolved spectra in a wavelength range from 220 to 340 nm. The reaction conditions are: [Pt(IV)] = 0.20 mM, $[CA]_{tot}$ = 2.00 mM, buffer of pH 4.42, 25.0°C, and 1.0 M ionic strength. Spectra were acquired at 3.3, 20, 40, 70, 100, 150, 200, 300, 400, 600, 800, 1000, 1500, 1995 ms [Color figure can be viewed at wileyonlinelibrary.com]

3.2 | Rapid scan spectra and rate law

To shed more light on the course of the redox reactions, time-resolved spectra were acquired in an HAc/NaAc buffer of pH 4.42 by use of the stopped-flow spectrometer, cf Figure 3. Characterized attributes in the spectra are that the absorption peak at about 236 nm and absorption shoulder between 260 and 280 nm retained unchanged and no new absorption band emerged, suggesting that neither a rapid substitution reaction on the Pt(IV) compound nor a strong association between CA and *cis*-$[Pt(NH_3)_2Cl_4]$ took place in the course of the redox reaction.

The influence of changing $[thiol]_{tot}$ on the reaction rates was investigated in an extended series of buffer solutions. In each buffer solution, the variation region of $[thiol]_{tot}$ was amended within the buffering capacity of that particular buffer, thus not causing any pH change of the buffered solutions. Consequently, a large body of kinetic data was collected for the oxidation reactions of both CA and Pen. Plots of k_{obsd} versus $[Pen]_{tot}$ in several buffers of different pH are shown in Figure 4, whereas the k_{obsd} versus $[CA]_{tot}$ plots are given in Figure S4 in the SM. Undoubtedly, these plots are linear and do not possess any significant intercepts within the experimental errors, revealing that the redox reactions are also first-order in $[thiol]_{tot}$. Therefore, the redox reactions follow overall second-order kinetics as expressed by Equation (2), where k' represents the observed second-order rate constant.

$$-\mathrm{d}\left[Pt(NH_3)_2Cl_4\right]/\mathrm{d}t = k_{obsd}\left[Pt(NH_3)_2Cl_4\right] = k'[thiol]_{tot}\left[Pt(NH_3)_2Cl_4\right] \quad (2)$$

Values of k' at different pHs were evaluated from the linear plots by a least-squares method and are summarized in Table S1 in the SM and are also shown in Figures 5 and 6.

3.3 | Stoichiometric ratios for the redox reactions

A spectrophotometric titration approach was opted to study the reaction stoichiometry of the present redox processes.[32–34] A series of reaction mixtures of *cis*-$[Pt(NH_3)_2Cl_4]$ with CA in a phosphate buffer of pH 6.29 were prepared, in which [Pt(IV)] = 0.20 mM was kept constant while $[CA]_{tot}$ was varied from 0 to 0.80 mM. Moreover, the absorption measurement at 265 nm for a reaction time of about 2 min was controlled for each reaction mixture avoiding the interference from the subsequence substitution reactions (vide supra). The measured absorption value as a function of $[CA]_{tot}$ is shown in Figure S5 in the SM; unambiguously the data points follow two straight crossing lines. A reaction ratio of $\Delta[Pt(IV)]$: $\Delta[CA]_{tot}$ = 0.20 mM:(0.43 ± 0.01) mM = 1:(2.15 ± 0.05)

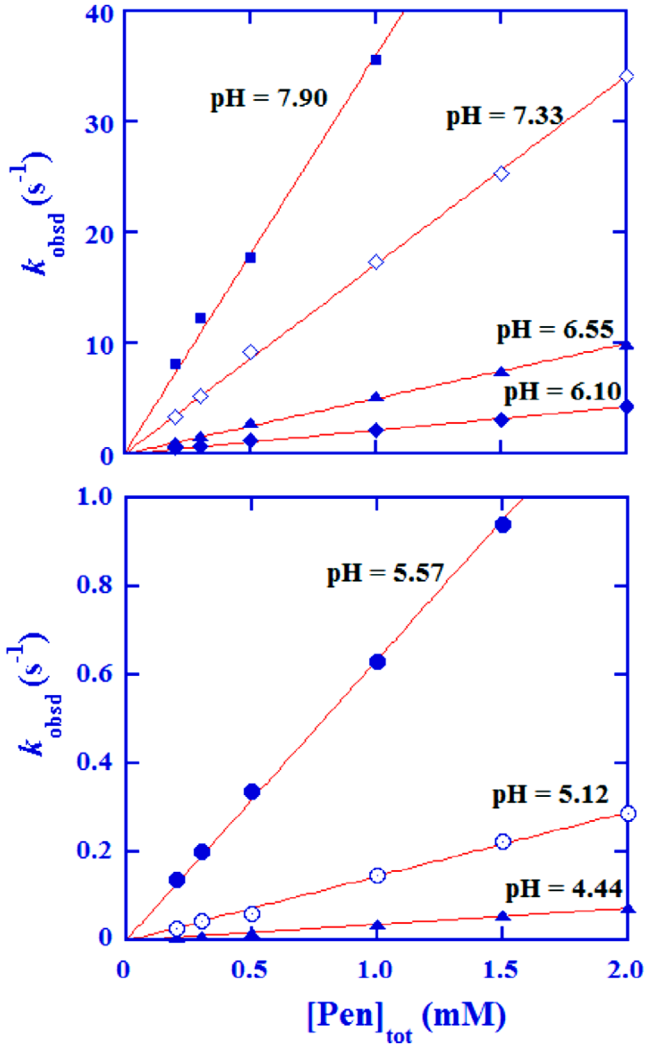

FIGURE 4 Plots of the pseudo first-order constant k_{obsd} versus $[Pen]_{tot}$ at 25.0°C and 1.0 M ionic strength [Color figure can be viewed at wileyonlinelibrary.com]

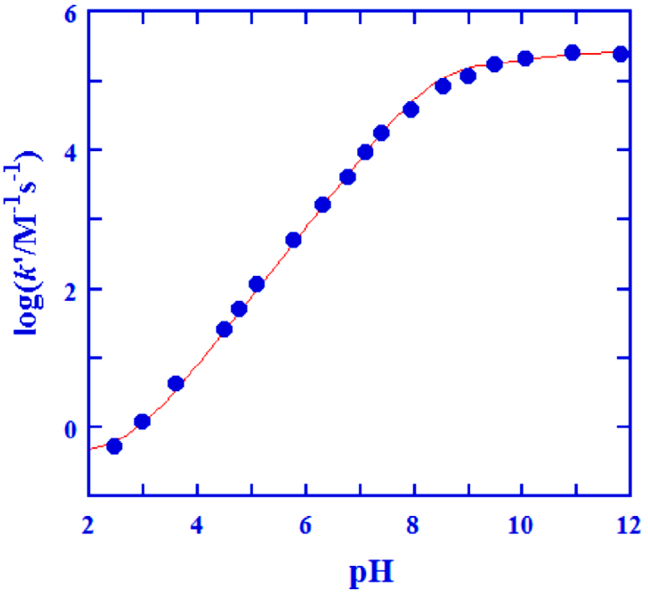

FIGURE 5 Observed second-order rate constant k' (in logarithmic scale) as a function of pH for the oxidation of CA by *cis*-$[Pt(NH_3)_2Cl_4]$ at 25.0°C and 1.0 M ionic strength. The solid curve was obtained by simulation of Equation (6) to the experimental data using a weighted nonlinear least-squares method [Color figure can be viewed at wileyonlinelibrary.com]

was estimated from the intersection point. Essentially, the estimated ratio is very close to a theoretical stoichiometry of 1:2 if CA was assumed to be oxidized to CA disulfide ($H_2NCH_2CH_2SSCH_2CH_2NH_2$ or CA-disulfide) as expressed by Equation (3):

$$[Pt(NH_3)_2Cl_4] + 2H_2NCH_2CH_2SH \rightarrow [Pt(NH_3)_2Cl_2] + H_2NCH_2CH_2SSCH_2CH_2NH_2 + 2HCl \quad (3)$$

A high-resolution mass spectrum, acquired for a reaction mixture of 10 mM CA and 1.0 mM *cis*-$[Pt(NH_3)_2Cl_4]$ in 1.0 mM HAc after a reaction time of about 0.5 h, is given in Figure S6 in the SM. From the peak assignments given in the figure legend, CA-disulfide was indeed the primary oxidation product of CA, justifying Equation (3). Under the pseudo first-order conditions with an excess of CA, deeper oxidations of CA probably yielding sulfenic acid and/or sulfinic acid were not observed, which is similar to the oxidations of glutathione and DL-homocysteine by Pt(IV) anticancer prodrugs.[18,19]

A similar spectrophotometric titration for the Pen oxidation was also carried out; Figure 7 shows the result together with the detailed experimental conditions. No doubt, the data points in the figure also follow two crossing straight lines, the intersection point renders a ratio of $\Delta[Pt(IV)]$: $\Delta[Pen]_{tot} = 0.30$ mM:(0.163 ± 0.006) mM = 1:(0.54 ± 0.02). This ratio, differentiating largely with the one obtained above for the CA oxidation, is in fact close to a 2:1 stoichiometry. Equation (4) is inferred to correspond to an ideal 2:1 stoichiometry:

$$H_2NCH(COOH)CMe_2SH + 2[Pt(NH_3)_2Cl_4] + 2H_2O \rightarrow H_2NCH(COOH)CMe_2SO_2H + 2[Pt(NH_3)_2Cl_2] + 4HCl \quad (4)$$

Equation (4) hypothesizes Pen-sulfinic acid ($H_2NCH(COOH)CMe_2SO_2H$ or Pen-SO_2H) being a major oxidation product of Pen. In order to confirm this hypothesis, a reaction mixture of 8 mM Pen with 1 mM *cis*-$[Pt(NH_3)_2Cl_4]$ was subjected to an ESI mass spectral analysis; both positive and negative ionization modes were performed. Figure S7 in the SM gives rise to the mass spectra together with the peak analysis in the figure legend. The analytic results unravel that two major oxidation

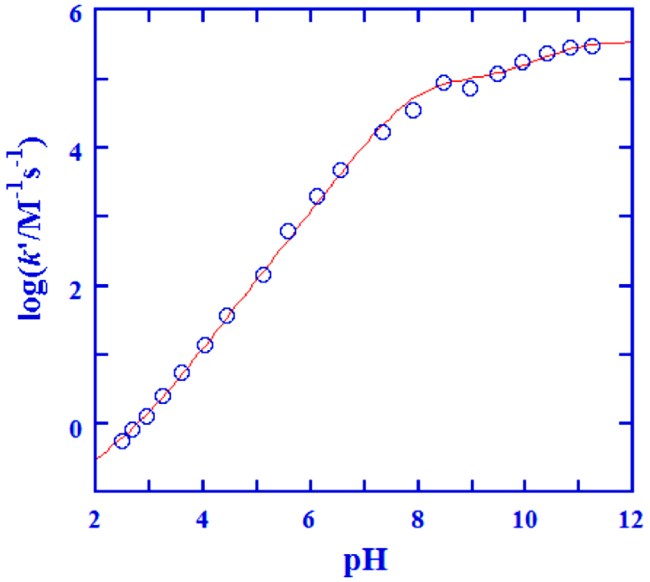

FIGURE 6 Observed second-order rate constant k' (in logarithmic scale) as a function of pH for the oxidation of Pen by *cis*-$[Pt(NH_3)_2Cl_4]$ at 25.0°C and 1.0 M ionic strength. The solid curve was acquired by simulation of Equation (8) to the experimental data using a weighted nonlinear least-squares method [Color figure can be viewed at wileyonlinelibrary.com]

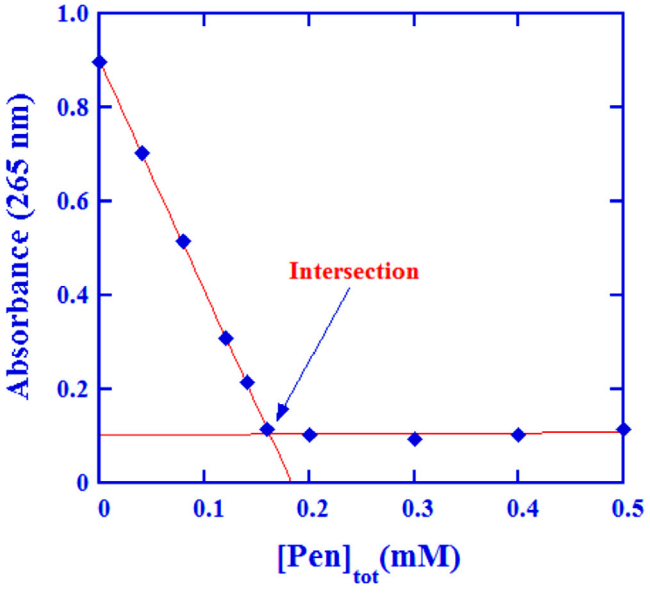

FIGURE 7 Spectrophotometric titration experiment: absorption value at 265 nm as function of $[Pen]_{tot}$ for a series of reaction mixtures of *cis*-$[Pt(NH_3)_2Cl_4]$ with Pen in a phosphate buffer of pH 6.29. In the reaction mixtures, [Pt(IV)] = 0.30 mM was maintained constant and $[Pen]_{tot}$ was varied from 0 to 0.50 mM; a reaction time of about 2 min was controlled for each of the reaction mixtures before the absorption measurement [Color figure can be viewed at wileyonlinelibrary.com]

products of Pen were generated in the reaction mixture: Pen-sulfinic acid and Pen-disulfide (Pen-S-S-Pen). However, the percentages of the two products cannot be evaluated from their peak heights since their mass spectral sensitivities are very different (the sulfinic acid form has a much lower sensitivity based on our experience). Hence, deeper oxidations than a disulfide were confirmed in the Pen oxidation in this work, which was not observed in the oxidations of other sterically unhindered thiol compounds by Pt(IV) compounds.[18,19]

3.4 | Mechanistic elucidations

All the reaction characters observed in the oxidation of CA by *cis*-$[Pt(NH_3)_2Cl_4]$ (including time-resolved spectra, overall second-order kinetics, and the reaction stoichiometry) are similar to those found in the oxidations of glutathionine and DL-homocysteine by Pt(IV) anticancer prodrugs.[18,19] Thus, a similar reaction mechanism is suggested as delineated in Scheme 1. In the scheme, reactions described by k_1–k_3 are the rate-determining steps, which have been interpreted in terms of a Cl^+ transfer from the Pt(IV) compound to the attacking sulfur atom of CA, resulting in formation of transient species chlorothiol and sulfenylchloride.[17–19] These transient species can be trapped rapidly by another CA molecule leading to formation of CA-disulfide (vide infra).[18,19]

In the oxidation of Pen by *cis*-$[Pt(NH_3)_2Cl_4]$, deeper oxidations engender a disparate stoichiometric ratio and two oxidation products of Pen. Except for these salient differences, the other kinetic characters are all similar to those found in the CA oxidation. When all these attributes are put together, a reaction mechanism is proposed as depicted in Scheme 2 for the Pen oxidation process involving rate-determining steps (i)-(iv). A transient species chlorothiol or sulfenylchloride is produced in each of the rate-determining steps. Each transient species is anticipated to be followed by a few fast reactions,[35,36] which are steps (v)-(viii) in Scheme 2 (with $^+H_3NCH(COO^-)CMe_2SCl$ (or Pen-SCl in short) generated in the reaction (iii) as an example). Specifically, step (v) is a trapping reaction of Pen-SCl by excess Pen in reaction solution[35,36]; this type of trapping reaction was very fast in the case of CA, but could be much slower in the case of Pen due to the highly sterically congested nature around the sulfur atom in both Pen-SCl and Pen. On the one hand, the trapping reaction brought about the product Pen-disulfide; on the other, a big portion of Pen-SCl had a good chance to undergo a hydrolytic reaction, leading to formation of another reactive species $^+H_3NCH(COO^-)CMe_2SOH$ (Pen-sulfenic acid), that is, the step (vi) in Scheme 2.[35,36] The doom of Pen-sulfenic acid was controlled by steps (vii) and (viii); step (vii) is another

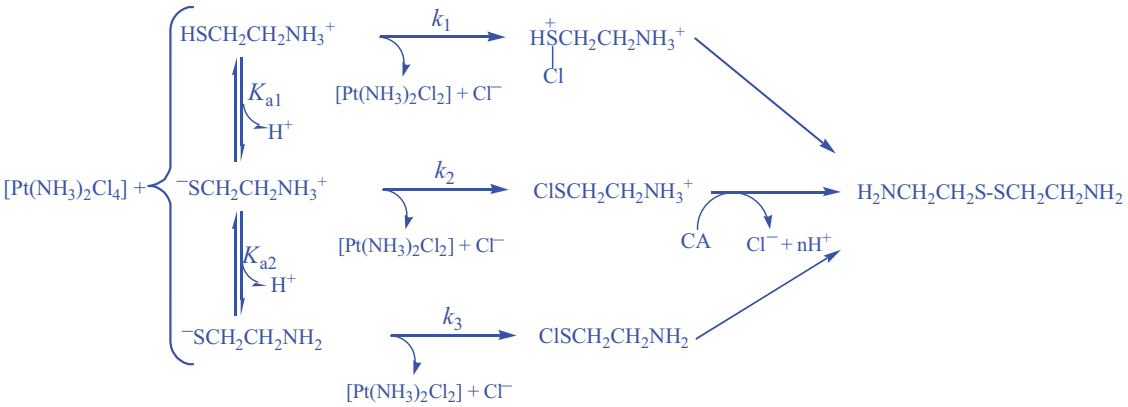

SCHEME 1 The reaction mechanism suggested for the oxidation of cysteamine by *cis*-$[Pt(NH_3)_2Cl_4]$ [Color figure can be viewed at wileyonlinelibrary.com]

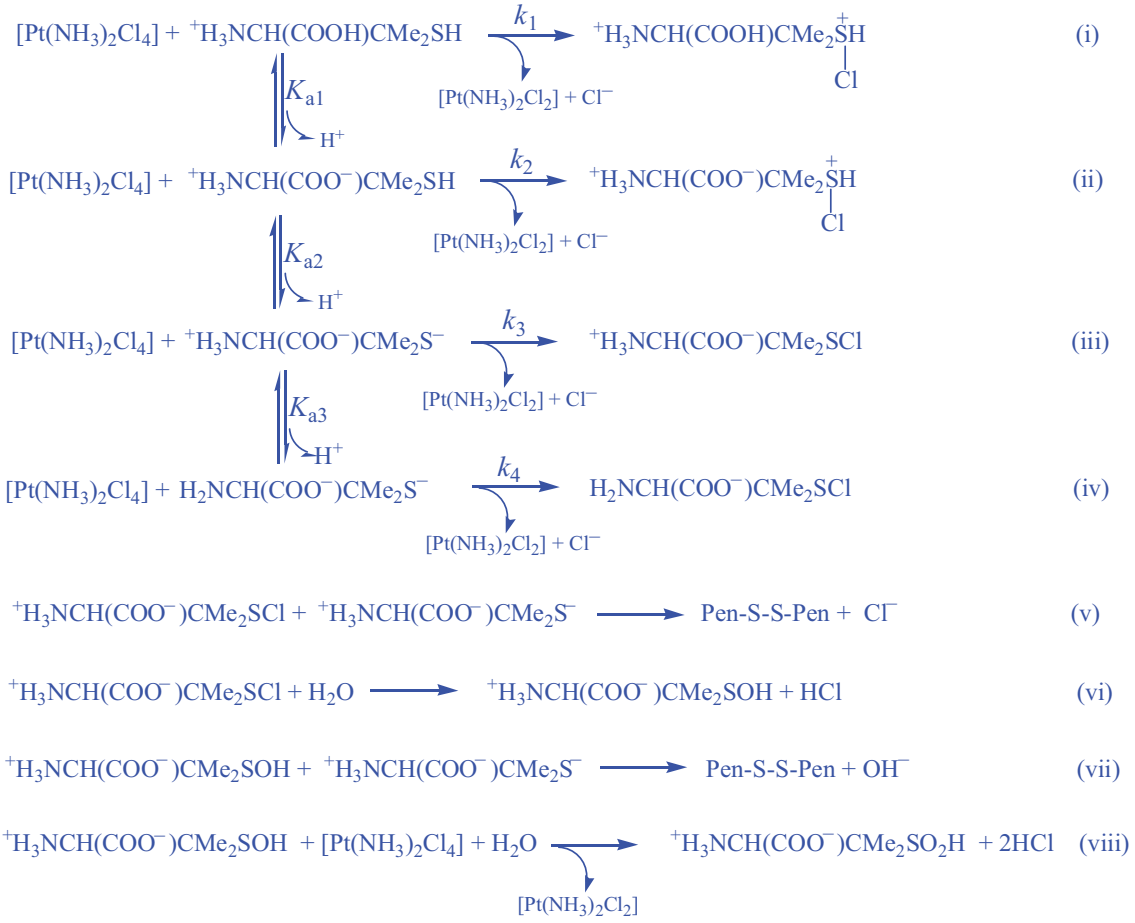

SCHEME 2 A schematic representation of the proposed reaction mechanism for the oxidation of D-penicillamine by *cis*-$[Pt(NH_3)_2Cl_4]$, in which reactions (i)-(iv) are the rate-determining steps [Color figure can be viewed at wileyonlinelibrary.com]

trapping reaction while step (viii) is a fast oxidation by another Pt(IV) molecule. By analogy, the highly steric congestion of Pen could make the rate of step (vii) slower significantly than that of step (viii). Step (vii) may only play a very minor role in the proposed mechanism but cannot be totally eliminated. It is thus understandable that the percentages of Pen-disulfide and Pen-sulfinic acid are largely determined by the relative rates of steps (v) and (viii). Nevertheless, step (viii) was apparently an open reaction route giving rise to a high portion of Pen-sulfinic acid and accounting for the stoichiometric ratio measured (vide supra).

TABLE 1 Rate constants of the rate-determining steps evaluated for the oxidations of cysteamine and D-penicillamine by *cis*-$[Pt(NH_3)_2Cl_4]$ at 25.0°C and ionic strength of 1.0 M

Thiol drug	k_m	Value (M^{-1} s^{-1})
CA	k_1	0.40 ± 0.05
	k_2	(1.85 ± 0.05) × 10^5
	k_3	(2.62 ± 0.09) × 10^5
Pen	k_1	Not observed
	k_2	0.43 ± 0.08
	k_3	(1.04 ± 0.05) × 10^5
	k_4	(3.53 ± 0.09) × 10^5

3.5 | Calculations of rate constants of the rate-determining steps

Equation (5) as the exact rate law was derived from Scheme 1, where K_{a1} and K_{a2} are the acid dissociation constants of CA and a_H stands for the proton activity, corresponding to the measured pH values (cf derivations of Equations 5-7 in the SM).

$$-\mathrm{d}[\mathrm{Pt(IV)}]/\mathrm{dt} = \frac{k_1 a_H{}^2 + k_2 K_{a1} a_H + k_3 K_{a1} K_{a2}}{a_H{}^2 + K_{a1} a_H + K_{a1} K_{a2}} [\mathrm{CA}]_{tot} [\mathrm{Pt(IV)}] \quad (5)$$

When Equation (5) is matched with Equation (2), Equation (6) is affordable:

$$k' = \frac{k_1 a_H{}^2 + k_2 K_{a1} a_H + k_3 K_{a1} K_{a2}}{a_H{}^2 + K_{a1} a_H + K_{a1} K_{a2}} \quad (6)$$

Simulation of Equation (6) to the k'-pH dependence data in Table S1 was performed by use of a weighted nonlinear least-squares method. In the simulation, k_1-k_3 were opted as adjustable parameters while the reported pK_a values of CA (pK_{a1} = 8.37 and pK_{a2} = 10.44 at 25.0°C and μ = 0.50 M[37]) were used as the direct inputs. The simulation conferred a good fit (cf Figure 5), concurrently generating the values of k_1-k_3, which are listed in Table 1.

According to Scheme 2, the rate expression for k' was deduced as Equation (7) (the derivation process is demonstrated in the SM):

$$k' = \frac{k_1 a_H{}^3 + k_2 K_{a1} a_H{}^2 + k_3 K_{a1} K_{a2} a_H + k_4 K_{a1} K_{a2} K_{a3}}{a_H{}^3 + K_{a1} a_H{}^2 + K_{a1} K_{a2} a_H + K_{a1} K_{a2} K_{a3}} \quad (7)$$

The dissociation constants of Pen were reported to be pK_{a1} = 1.9, pK_{a2} = 7.92, and pK_{a3} = 10.50 at 25.0°C and μ = 1.0 M.[38] When Equation (7) was employed to simulate the k'-pH dependence data in Table S1 in the SM and the pK_a values were treated as the fixed constants, it turned out that the k_1 value was indeterminate (or not observed). Consequently, Equation (7) was reduced to Equation (8) by exclusion of the k_1-term in Equation (7).

$$k' = \frac{k_2 K_{a1} a_H{}^2 + k_3 K_{a1} K_{a2} a_H + k_4 K_{a1} K_{a2} K_{a3}}{a_H{}^3 + K_{a1} a_H{}^2 + K_{a1} K_{a2} a_H + K_{a1} K_{a2} K_{a3}} \quad (8)$$

The simulation of the data by Equation (8) was then executed, offering an essentially excellent fit, cf Figure 6; the k_2-k_4 values secured by the simulation are also summarized in Table 1.

The excellent fits in Figures 5 and 6 lend a strong support to the reasonableness of the proposed reaction mechanisms. The rate-determining steps in Schemes 1 and 2 are anticipated to take place via a bridge formation between one of the *trans*-coordinated chlorides in *cis*-$[Pt(NH_3)_2Cl_4]$ and the attacking sulfur atom of CA or Pen whereas the bridge formation leads consequently to a Cl^+ transfer from the Pt(IV) center to the sulfur atom.[17,35] Moreover, recent theoretical calculations on the reductions of *trans*-dichloro-platinum(IV) compounds clearly bolster the above Cl^+ transfer mechanism.[39,40] Among the oxidants exploited for the oxidations of the two drugs,[10–15] the chloramine was the only one in its reaction mechanism involving a Cl^+ transfer as that in the present reaction systems,[11] but the chloramine oxidations were slower in rates.

3.6 | An alternative reaction mechanism

An alternative reaction mechanism for the oxidation of CA by *cis*-$[Pt(NH_3)_2Cl_4]$ is also suggested, as delineated in Figure S8 in the SM. This mechanism involves formation of free radicals on the sulfur atom from CA species and generation of a Pt(III) intermediate in the rate determining-steps (a)-(c); Pt(III) is hardly holding the same configuration as *cis*-$[Pt(NH_3)_2Cl_4]$ and is thus presumed as $[Pt(NH_3)_2Cl_3]$. If we assume that the Pt(III) intermediate is very active, it rapidly reacts with the thiol species in excess; with $^-SCH_2CH_2NH_2$ as an example, this rapid reaction is reaction (d) in Figure S8 generating another free radical•$SCH_2CH_2NH_2$. Reaction (e) in Figure S8 is the rapid combination of two free radicals leading to formation of final product. Based on the reaction mechanism in Figure S8 and on the assumptions, the rate Equation (5) is also obtainable. In such case, the values of rate constants k_1-k_3 in Table 1 have a different meaning.

In fact, the assumptions of formation of the Pt(III) intermediate and of Pt(III) being very reactive in the mechanism are hardly finding supports from the experi-

ments in this work. If the rate-determining steps involve single-electron transfer processes, the speeds of these processes are expected to be closely related to the redox potentials of the Pt(IV) complexes; the higher the redox potential of Pt(IV) complex, the higher of the electron-transfer speed. Our earlier works demonstrated that *cis*,*trans*-$[Pt(NH_3)_2Cl_2Br_2]$ and *trans*-$[PtBr_2(CN)_4]^{2-}$, having lower redox potentials than *cis*-$[Pt(NH_3)_2Cl_4]$ and *trans*-$[PtCl_2(CN)_4]^{2-}$, respectively, are reduced much faster.[17,32] Hence, our earlier findings are against the reaction mechanism illustrated in Figure S8.[17,32]

3.7 | Analysis of reactivity of the drug species

The rate constants in Table 1 demonstrate a huge reactivity difference between the thiol and thiolate forms of the drugs in the reduction of *cis*-$[Pt(NH_3)_2Cl_4]$ (about 10^5 times), accounting for the large pH dependence of the observed second-order rate constants in Table S1. For a straight visualization, Figures S9 and S10 in the SM were constructed by use of the dissociation constants of CA and Pen and of the rate constants of rate-determining steps in Table 1.[18,19] The diagrams demonstrate the molar fraction versus pH and the reactivity fraction versus pH distribution diagrams respectively for the oxidations of CA and Pen. It is readily observed that the species $^{-}SCH_2CH_2NH_3^{+}$ of CA and the species $^{+}H_3NCH(COO^{-})CMe_2S^{-}$ of Pen play a predominant role in the reduction of *cis*-$[Pt(NH_3)_2Cl_4]$ from pH 5 to 8, which is also a pharmacologically critical pH region for functions for most of drugs.

4 | CONCLUSION

The oxidations of CA and Pen by *cis*-$[Pt(NH_3)_2Cl_4]$ were characterized kinetically and mechanistically over a wide pH range in this work; they strictly followed second-order kinetics and similar rate laws, but proceeded via disparate stoichiometric ratios and rendered different patterns of oxidation products. The similarities and differences are well rationalized in terms of the proposed reaction mechanisms, demonstrating how deeper oxidations of Pen by the Pt(IV) prodrug took place, which were caused by the sterically hindered congestion of the thiol group in Pen. The mechanisms elucidated in this work are clearly convincing and provide a good reference when new antioxidative reactions related to their pharmacological processes are investigated in the future. Moreover, it was revealed that the species $^{-}SCH_2CH_2NH_3^{+}$ of CA and the species $^{+}H_3NCH(COO^{-})CMe_2S^{-}$ of Pen played a predominant role in the reduction of *cis*-$[Pt(NH_3)_2Cl_4]$ from pH 5 to 8, which is also a medically critical pH region for functions for most of drugs.

CONFLICT OF INTEREST

The authors declare no conflict of interest.

DATA AVAILABILITY STATEMENT

The data that support the findings of this study are openly available in at https://doi.org/[doi], reference number [reference number].

ORCID

Tiesheng Shi https://orcid.org/0000-0002-0767-6324

REFERENCES

1. Kleta R, Gahl WA. Pharmacological treatment of nephropathic cystinosis with cysteamine. *Expert Opin Pharacother*. 2004;5:2255-2262.
2. Medic G, van der Weijden M, Karabis A, Hemels MA. Systematic literature review of cysteamine bitartrate in the treatment of nephropathic cystinosis. *Curr Med Res Opin*. 2017;33:2065-2076.
3. Besouw M, Masereeuw R, van den Heuvel L, Levtcheko E. Cysteamine: an old drug with new potential. *Drug Disc Today*. 2013;18:758-792.
4. Eidelman C, Lowry JA. D-penicillamine. In: Brent J, ed. *Critical Care Toxicology*. Springer International Publishing AG; 2016:1-7.
5. Grazyna G, Agata K, Adam P, et al. Treatment with D-penicillamine or zinc sulphate affects copper metabolism and improves but not normalizes antioxidant capacity parameters in Wilson disease. *Biometals*. 2014;27:207-215.
6. Wadhwa S, Mumpper RJ. D-penicillamine and other low molecular weight thiols: review of anticancer effects and related mechanisms. *Cancer Lett*. 2013;337:8-21.
7. Zhang ZY, Yang MF, Wang T, et al. Cysteamine alleviates early brain injury via reducing oxidative stress and apoptosis in a rat experimental subarachnoid hemorrhage model. *Cell Mol Neurobiol*. 2015;35:543-553.
8. Daryl M, Okamura DM, Bahrami NM, et al. Cysteamine modulates oxidative stress and blocks myofibroblast activity in CKD. *J Am Soc Nephrol*. 2014;25:43-54.
9. Squitti R, Rossini PM, Cassetta E, Moffa F, et al. D-Penicillamine reduces serum oxidative stress in Alzheimer's disease patients. *Eur J Clin Invest*. 2002;32:51-59.
10. Mottley C, Toy K, Mason RP. Oxidation of thiol drugs and biochemicals by the lactoperoxidase/hydrogen peroxide system. *Mol Pharmacol*. 1987;31:417-421.
11. Peskin AV, Winterbourn CC. Kinetics of the reactions of hypochlorous acid and amino acid chloramines with thiols, methionine, and ascorbate. *Free Radic Biol Med*. 2001;30:572-579.
12. Hu TM, Ho SC. Kinetics of redox interaction between cytochrome c and thiols. *J Med Sci*. 2011;31:109-115.
13. Gupte A, Mumper RJ. An investigation into copper catalyzed D-penicillamine oxidation and subsequent hydrogen peroxide generation. *J Inorg Biochem*. 2007;101:594-602.
14. Morakinyo MK, Chikwana E, Simoyi RH. Oxyhalogen–sulfur chemistry – Kinetics and mechanism of the bromate oxidation of cysteamine. *Can J Chem*. 2008;86:416-425.

15. Chipiso K, Simoyi RH. Kinetics and mechanism of oxidation of D-penicillamine in acidified bromate and aqueous bromine. *Aust J Chem*. 2016;69:1305-1313.
16. Huo S, Shi H, Liu D, et al. Kinetics and mechanism of reactions of the drug tiopronin with platinum(IV) complexes. *J Inorg Biochem*. 2013;125:9-15.
17. Dong J, Ren Y, Huo S, et al. Reduction of ormaplatin and cis-diamminetetrachloroplatinum(IV) by ascorbic acid and dominant thiols in human plasma: kinetic and mechanistic analyses. *Dalton Trans*. 2016;45:11326-11337.
18. Dong J, Huo S, Shen S, Xu J, Shi T, Elding LI. Reactivity of the glutathione species towards the reduction of ormaplatin (or tetraplatin). *Bioorg Med Chem Lett*. 2016;26:4261-4266.
19. Tian H, Dong J, Che X, Xu L, Shi H, Shi T. Reduction of cisplatin and carboplatin Pt(IV) prodrugs by homocysteine: kinetic and mechanistic investigations. *Int J Chem Kinet*. 2017;49:681-689.
20. Dong J, Ren Y, Sun S, et al. Kinetics and mechanism for oxidation of the anti-tubercular prodrug isoniazid and its analog by iridium(IV) as models for biological redox systems. *Dalton Trans*. 2017;46:8377-8386.
21. Hall MD, Daly HL, Zhang JZ, et al. Quantitative measurement of the reduction of platinum (IV) complexes using X-ray absorption near-edge spectroscopy (XANES). *Metallomics*. 2012;4:568-575.
22. Johnstone TC, Alexander SM, Wilson JJ, Lippard SJ. Oxidative halogenation of cisplatin and carboplatin: synthesis, spectroscopy, and crystal and molecular structures of Pt(IV) prodrugs. *Dalton Trans*. 2015;44:119-129.
23. Nakai T, Ando M, Okamoto Y, Ueda K, Kojima N. Modulation of oxidative DNA damage and DNA-crosslink formation induced by cis-diamminetetrachloroplatinum(IV) in the presence of endogenous reductants. *J Inorg Biochem*. 2011;105:1-5.
24. Weaver EL, Bose RN. Platinum(II) catalysis and radical intervention in reductions of platinum(IV) antitumor drugs by ascorbic acid. *J Inorg Biochem*. 2003;95:231-239.
25. McCormick MC, Keijzer K, Polavarapu A, Schultz FA, Baik MH. Understanding intrinsically irreversible, non-nernstian, two-electron redox processes: a combined experimental and computational study of the electrochemical activation of platinum(IV) antitumor prodrugs. *J Am Chem Soc*. 2014;136:8992-8990.
26. Chen SJ, Kuo CC, Pan HY, Tsou TC, Yeh SC, Chang JY. Mechanistic basis of a combination D-penicillamine and platinum drugs synergistically inhibits tumor growth in oxaliplatin-resistant human cervical cancer cells in vitro and in vivo. *Biochem Pharmacol*. 2015;95:28-37.
27. Taylor JE, Yan JF, Wang JI. The iron (III)-catalyzed oxidation of cysteine by molecular oxygen in the aqueous phase. An example of a two-thirds-order reaction. *J Am Chem Soc*. 1966;88:1663-1667.
28. Kachur AV, Koch CJ, Biaglow JE. Mechanism of copper-catalyzed oxidation of glutathione. *Free Radic Res*. 1998;28:259-269.
29. Ehrenberg L, Harms-Ringdahl M, Fedorcsak I, Granath F. Kinetics of the copper-and iron-catalyzed oxidation of cysteine by dioxygen. *Acta Chem Scand*. 1989;43:177-187.
30. Zhang X. Oxidations of benzhydrazide and phenylacetic hydrazide by hexachloroiridate (IV): reaction mechanism and structure–reactivity relationship. *Molecules*. 2020;25:308.
31. Dedon PC, Borch RF. Characterization of the reactions of platinum antitumor agents with biologic and nonbiologic sulfur-containing nucleophiles. *Biochem Pharmacol*. 1987;36:1955-1964.
32. Liu C, Xu L, Tian H, Yao H, Elding LI, Shi T. Kinetics and mechanism for reduction of anticancer model compounds by Se-methyl L-selenocysteine. Comparison with L-selenomethionine. *J Mol Liq*. 2018;271:838-843.
33. Xu L, Tian H, Yao H, Shi T. New kinetic and mechanistic findings in the oxidation of hydroxylamine by cerium(IV) in perchloric acid. *Int J Chem Kinet*. 2018;50:856-862.
34. Liu Y, Tian H, Xu L, et al. Investigations of the kinetics and mechanism of reduction of a carboplatin Pt(IV) prodrug by the major small-molecule reductants in human plasma. *Int J Mol Sci*. 2019;20:5660.
35. Shi T, Berglund J, Elding LI. Kinetics and mechanism for reduction of *trans*-dichorotetracyanoplatinate(IV) by tioglycolic acid, L-cysteine, DL-penicillamine, and glutathione in aqueous solution. *Inorg Chem*. 1996;35:3498-3503.
36. Turell L, Radi R, Alvarez B. The thiol pool in human plasma: the central contribution of albumin to redox processes. *Free Radic Biol Med*. 2013;65:244-253.
37. Connett PH, Wetterhahn KE. Reaction of chromium(VI) with thiols: pH dependence of chromium(VI) thio ester formation. *J Am Chem Soc*. 1986;108:1842-1847.
38. Smith RM, Martell AE. *Critical Stability Constants*. New York: Plenum Press; 1989. 2nd Suppl., Page 20.
39. Chipman A, Yates BF, Canty AJ, Ariafard A. Reduction of a platinum(iv) prodrug model by sulfur containing biological reductants: computational mechanistic elucidation. *Chem Commun*. 2018;54:10491-10494.
40. Wang J, Yao H, Lu T, et al. Spectroscopic, kinetic, and theoretical analyses of oxidation of DL-ethionine by Pt(IV) anticancer model compounds. *Spectrochim Acta A*. 2019;223:117328.

SUPPORTING INFORMATION

Additional supporting information may be found online in the Supporting Information section at the end of the article.

How to cite this article: Zhou L, Li T, Sun Y, et al. Mechanistic scrutiny of the oxidations of thiol-containing drugs cysteamine and D-penicillamine by *cis*-diamminetetrachloroplatium(IV). *Int J Chem Kinet*. 2020;1-10. https://doi.org/10.1002/kin.21464